James E. Dunn[1] *and Tong Chen*[1]

Critical Evaluation of the Diffusion Hypothesis in the Theory of Porous Media Volatile Organic Compound (VOC) Sources and Sinks

REFERENCE: Dunn, J. E. and Chen, T., **"Critical Evaluation of the Diffusion Hypothesis in the Theory of Porous Media Volatile Organic Compound (VOC) Sources and Sinks,"** *Modeling of Indoor Air Quality and Exposure, ASTM STP 1205*, Niren L. Nagda, Ed., American Society for Testing and Materials, Philadelphia, 1993, pp. 64–80.

ABSTRACT: Recently, reports by both the U.S. Environmental Protection Agency (EPA) and a study committee of the Commission of the European Communities have alluded to diffusion mechanisms that may play a role in Volatile Organic Compound (VOC) interactions with indoor sinks. This paper proposes three alternative, diffusion-limited mathematical models to account for this interaction, using the linear isotherm model as a reference point. Their taxonomy is keyed to the nature of the vapor-sink interface. While the linear isotherm model gave an adequate description of data when a pillow-sink was challenged with ethylbenzene, a new single-parameter diffusion model gave a much improved description of data when the same pillow-sink was challenged with perchloroethylene. A hybrid, sorption/desorption, diffusion-limited model was the only plausible model when a carpet-sink was challenged with ethylbenzene. Some new computational aids, particularly interval-weighted least squares, are introduced in the context of model validation.

KEY WORDS: mathematical model, weighted least squares, linear isotherm, pillow, carpet, ethylbenzene, perchloroethylene, indoor air

The existence of indoor, re-emitting sinks for volatile organic compounds (VOC) is now well documented by Berglund et al. [*1*], Nielsen [*2*], Nielsen [*3*], and Tichenor et al. [*4*], among others, and an active, small-chamber testing program of this phenomenon is underway [*5*]. However, the mechanisms by which VOC sinks operate are not well understood.

Recently, both the U.S. Environmental Protection Agency (EPA) [*6*] and the Commission of the European Communities [*7*] published guidelines for use of small environmental test chambers to characterize organic emissions from indoor materials and products. Both reports list three fundamental processes that are thought to control the rate of emissions: (1) surface evaporative mass transfer, (2) surface desorption, and (3) diffusion within the material. Models based on the first two phenomena have been used with varying success to characterize volatile organic compound (VOC) sources [*8, 9*] and sinks [*5*]. While a diffusion limitation often has been alluded to in order to account for not infrequently observed VOC decay curves that are slower than negative exponential, mathematical formulations of this concept have been limited to linearized approximations of diffusion across the boundary layer [*10,11*]. Consistent with the need stated by Axley [*10*] for physical models based on diffusion processes in a porous media, we propose here several potential

[1]Professor and chairman, and research assistant, respectively, University of Arkansas, Statistics Division, Department of Mathematical Sciences, Fayetteville, AR 72701. Research by the senior author was supported under the United States Environmental Protection Agency (USEPA) Cooperative Agreement CR-818520-01-0.

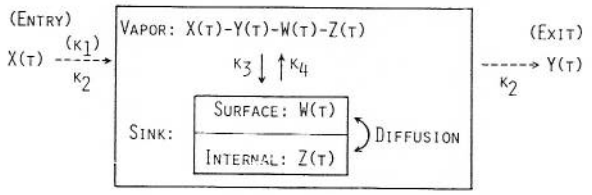

FIG. 1—*Mass balance schematic of alternative VOC sink models.*

models that account for diffusion-limited VOC sink effects and present statistical evidence that we have used to discriminate among their alternative forms.

All models presented here are unified models in the sense that they apply to the whole course of accumulation and decay. In actual applications of chamber studies to indoor air quality (IAQ), we will never be able to predict when we will be in an accumulation or decay phase, so that the same model must apply to both.

Admittedly, the functional forms of some of these models are formidable, often involving complex roots of a polynomial equation. However, since our aim was to attempt validation of these models exactly as postulated, we avoided simplifying approximations. The reader may wish to focus on the model assumptions that are given in the following section, rather than being immediately dismayed by the mathematical complexities of Table 1.

In what follows, we suppose that clean air is swept through a well-mixed test chamber of volume V containing a sink of surface area A at a constant rate of k_2 air exchanges per time unit. At time $t = 0$, VOC is introduced into the initially VOC-free test chamber at a constant rate of k_1 mass units per time unit. At time $t = t_0$, this source of VOC is removed and the VOC concentration is allowed to decay. The only available measurement is that of chamber, vapor-phase concentration, $C(t)$ at any time $t > 0$.

The following four, unified models for $C(t)$ were developed:

(1) linear adsorption isotherm model,
(2) diffusion-limited model with finite transfer coefficient,
(3) diffusion-limited model with an infinite transfer coefficient, and
(4) hybrid, diffusion-limited model with sorption phenomena at the vapor/sink interface.

The distinctions among these models are best visualized by an examination of a mass balance schematic given in Fig. 1

where

$X(t)$ = VOC mass introduced into the test chamber by time t,
$Y(t)$ = VOC mass swept from the test chamber by time t,
$W(t)$ = VOC mass subject to desorption at time t,
$Z(t)$ = VOC mass interior to the sink, subject to diffusion at time t;
k_3 = sorption rate constant for the sink,
k_4 = desorption rate constant for the sink,
$U(x, t)$ = VOC concentration at distance x interior to the sink at time t,
E = finite transfer coefficient between the vapor phase and the sink, and
k = diffusion coefficient of the VOC within the sink,

in terms of internally consistent units. $W(t)$ is associated with the surface of the sink, while $Z(t)$ occupies the porous structure. C_0, W_0, and Z_0 denote, respectively, initial values of $C(t)$, $W(t)$, and

$Z(t)$ at time $t = 0$. The function $G(t) = k_1 I_{(0,t_0)}(t)$ will be used throughout to describe an interrupted input in terms of an indicator function I.

Mathematical Models for Sinks

Linear Isotherm Model

Suppose that there is no penetration of VOC into the sink so that $Z(t) = 0$ for $t \geqq 0$. Mass balance is described by thin-film sorption properties of the sink as follows

$$\frac{dX}{dt} = G(t) \tag{1}$$

$$\frac{dY}{dt} = k_2(X - Y - W) = k_2 VC \tag{2}$$

$$\frac{dW}{dt} = k_3(X - Y - W) - \underset{\text{(sorption)}}{} \quad \underset{\text{(desorption)}}{k_4 W} = k_3 VC - k_4 W \tag{3}$$

from which chamber vapor phase concentration is defined by

$$\frac{dC}{dt} = \frac{1}{V}\left[\frac{dX}{dt} - \frac{dY}{dt} - \frac{dW}{dt}\right] = \frac{G(t)}{V} - (k_2 + k_3)C + \frac{k_4 W}{V} \tag{4}$$

This model has appeared in Dunn and Tichenor [*8*], and in reparameterized form in Tichenor et al. [*5*], though in neither case as a unified model. Equating Eq 3 to zero yields the steady state, linear isotherm, $W = K_p C$, in terms of the partition coefficient [*10*] $K_p = k_3 V/k_4$. Solutions $C(t)$ and $W(t)$ are given in Table 1.

Diffusion-Limited Models

Suppose that the surface of the sink does not provide a physical barrier to VOC penetration, but that once a VOC molecule penetrates the surface of the sink, its movement is controlled by the 1-dimensional diffusion equation

$$U_t(x, t) = kU_{xx}(x, t),\ x \geqq 0, \tag{5}$$

where the orientation of the x axis is taken so that the vapor phase is to the left of the origin at $x = 0$ and the sink is to the right. Flux of VOC/unit surface area, immediately to the right of the interface, is $-kU_x(+0, t)$. If no sorption occurs on the surface of the sink, so that $W(t) = 0$ for $t \geqq 0$, then, in addition to Eq 1, mass balance equations are given by

$$\frac{dY}{dt} = k_2(X - Y - Z) = k_2 VC \tag{6}$$

$$\frac{dZ}{dt} = -kAU_x(+0, t) \tag{7}$$

and chamber vapor phase concentration is defined by

$$\frac{dC}{dt} = \frac{G(t)}{V} - k_2 C + \frac{kA}{V} U_x(+0, t) \tag{8}$$

An initial model, which we termed the K & E diffusion model, resulted from imposing initial and boundary conditions

$$\#1 \quad U(x, 0) = 0 \text{ for } x \geqq 0 \quad \text{(the sink is empty initially)} \tag{9}$$

$$\#2 \quad \lim_{x \to \infty} U(x, t) = 0 \text{ for all } t \quad \text{(the sink is nonsaturable)} \tag{10}$$

$$\#3 \quad kU_x(+0, t) = E[U(+0, t) - C(t)] \quad \left(\begin{matrix}\text{flux is driven by concentration} \\ \text{difference at the interface}\end{matrix}\right) \tag{11}$$

However, in attempts to fit this model to actual data, E was estimated to be very large, for example, of order 1.0×10^{22} m/100 h. Therefore, we supposed that the transfer coefficient must dominate the flux rate and arrived at an alternative to boundary condition #3, namely.

$$\#3 \quad \lim_{E \to \infty} \frac{kU_x(\pm 0, t)}{E} = 0 \rightarrow U(+0, t) = C(t). \tag{12}$$

This seems reasonable as it corresponds to no discontinuity in VOC concentration at the interface. The result is termed a K-diffusion model. Solutions for $C(t)$, $Z(t)$, and $U(x, t)$ are given in Table 1 in terms of the complementary error function

$$\operatorname{erfc}(x) = \frac{2}{\sqrt{\pi}} \int_x^\infty e^{-r^2} dr \tag{13}$$

Hybrid Diffusion Model

Suppose that the only pathway by which VOC may enter or leave a diffusion-limited sink is through sorbed material on the surface of the sink. Then, in addition to Eq 1, the following mass balance equations result

$$\frac{dY}{dt} = k_2(X - Y - W - Z) = k_2 VC \tag{14}$$

$$\frac{dW}{dt} = k_3(X - Y - W - Z) + AkU_x(+0, t) - k_4 W = k_3 VC + AkU_x(+0, t) - k_4 W \tag{15}$$

(sorption) (diffusion) (desorption)

where

$$Z(t) = A \int_0^\infty U(x, t) dx \tag{16}$$

TABLE 1—*Voc sink models arising from alternative mass balance assumptions.*

Linear Isotherm Model

$$C(t)=\frac{k_1}{k_2V}\left\{1+\frac{(k_2+\theta_2)e^{\theta_1 t}-(k_2+\theta_1)e^{\theta_2 t}}{\theta_1-\theta_2}\right\}-\frac{k_1}{k_2V}\left\{1+\frac{(k_2+\theta_2)e^{\theta_1(t-t_o)}-(k_2+\theta_1)e^{\theta_2(t-t_o)}}{\theta_1-\theta_2}\right\}I_{(t_o,\infty)}(t)+W_o\frac{k_4(e^{\theta_1 t}-e^{\theta_2 t})}{V(\theta_1-\theta_2)}+C_o\frac{(k_4+\theta_1)e^{\theta_1 t}-(k_4+\theta_2)e^{\theta_2 t}}{\theta_1-\theta_2},$$

$$W(t)=k_1k_3\left\{\frac{1}{k_2k_4}+\frac{e^{\theta_1 t}}{\theta_1(\theta_1-\theta_2)}-\frac{e^{\theta_2 t}}{\theta_2(\theta_1-\theta_2)}\right\}-k_1k_3\left\{\frac{1}{k_2k_4}+\frac{e^{\theta_1(t-t_o)}}{\theta_1(\theta_1-\theta_2)}-\frac{e^{\theta_2(t-t_o)}}{\theta_2(\theta_1-\theta_2)}\right\}I_{(t_o,\infty)}(t)$$
$$+C_ok_3V\frac{(e^{\theta_1 t}-e^{\theta_2 t})}{\theta_1-\theta_2}+W_o\frac{k_3k_4}{\theta_1-\theta_2}\left\{\frac{e^{\theta_1 t}}{k_4+\theta_1}-\frac{e^{\theta_2 t}}{k_4+\theta_2}\right\},$$

where $\theta_1,\ \theta_2=\{-(k_2+k_3+k_4)\pm[(k_2+k_3+k_4)^2-4k_2k_4]^{1/2}\}/2$[a].

K-diffusion Model ($E\to\infty$)

$$C(t)=\frac{k_1}{V}\left\{\frac{1}{k_2}+\frac{e^{\theta_1^2 t}\,\mathrm{erfc}(-\theta_1\sqrt{t})}{\theta_1(\theta_1-\theta_2)}-\frac{e^{\theta_2^2 t}\,\mathrm{erfc}(-\theta_2\sqrt{t})}{\theta_2(\theta_1-\theta_2)}\right\}-\frac{k_1}{V}\left\{\frac{1}{k_2}+\frac{e^{\theta_1^2(t-t_o)}\,\mathrm{erfc}(-\theta_1\sqrt{t-t_o})}{\theta_1(\theta_1-\theta_2)}-\frac{e^{\theta_2^2(t-t_o)}\,\mathrm{erfc}(-\theta_2\sqrt{t-t_o})}{\theta_2(\theta_1-\theta_2)}\right\}I_{(t_o,\infty)}(t)$$
$$+C_o\left\{\frac{\theta_1 e^{\theta_1^2 t}\,\mathrm{erfc}(-\theta_1\sqrt{t})-\theta_2 e^{\theta_2^2 t}\,\mathrm{erfc}(-\theta_2\sqrt{t})}{\theta_1-\theta_2}\right\},$$

$$Z(t)=\frac{Ak_1\sqrt{k}}{V}\left\{\frac{2\sqrt{t}}{k_2\sqrt{\pi}}-\frac{A\sqrt{k}}{k_2^2V}+\frac{e^{\theta_1^2 t}\,\mathrm{erfc}(-\theta_1\sqrt{t})}{\theta_1^2(\theta_1-\theta_2)}-\frac{e^{\theta_2^2 t}\,\mathrm{erfc}(-\theta_2\sqrt{t})}{\theta_2^2(\theta_1-\theta_2)}\right\}-\left\{\frac{2\sqrt{t-t_o}}{k_2\sqrt{\pi}}-\frac{A\sqrt{k}}{k_2^2V}+\frac{e^{\theta_1^2(t-t_o)}\,\mathrm{erfc}(-\theta_1\sqrt{t-t_o})}{\theta_1^2(\theta_1-\theta_2)}-\frac{e^{\theta_2^2(t-t_o)}\,\mathrm{erfc}(-\theta_2\sqrt{t-t_o})}{\theta_2^2(\theta_1-\theta_2)}\right\}$$
$$\cdot\frac{Ak_1\sqrt{k}}{V}I_{(t_o,\infty)}(t)+C_o\frac{A\sqrt{k}}{\theta_1-\theta_2}\left\{e^{\theta_1^2 t}\,\mathrm{erfc}(-\theta_1\sqrt{t})-e^{\theta_2^2 t}\,\mathrm{erfc}(-\theta_2\sqrt{t})\right\}+Z_o,$$

$$U(x,t)=\frac{k_1}{V}\left\{\frac{\mathrm{erfc}[x/(2\sqrt{kt})]}{k_2}+\sum_{i=1}^{2}\frac{(-1)^{1-1}e^{-x\theta_1/\sqrt{k}+\theta_1^2 t}}{\theta_1(\theta_1-\theta_2)}\,\mathrm{erfc}[x/(2\sqrt{kt})-\theta_1\sqrt{t}]\right\}-\frac{k_1}{V}\left\{\frac{\mathrm{erfc}[x/(2\sqrt{k(t-t_o)})]}{k_2}+\sum_{i=1}^{2}\frac{(-1)^{1-1}e^{-x\theta_1/\sqrt{k}+\theta_1^2(t-t_o)}}{\theta_1(\theta_1-\theta_2)}\,\mathrm{erfc}[x/(2\sqrt{k(t-t_o)})-\theta_1\sqrt{t-t_o}]\right\}I_{(t_o,\infty)}(t)$$
$$+C_o\sum_{i=1}^{2}\frac{(-1)^{1-1}\theta_1 e^{-x\theta_1/\sqrt{k}+\theta_1^2 t}}{\theta_1-\theta_2}\,\mathrm{erfc}[x/(2\sqrt{kt})-\theta_1\sqrt{t}],$$

where $\theta_1,\ \theta_2=\{-A\sqrt{k}/v\pm[A^2k/V^2-4k_2]^{1/2}\}/2$[b].

TABLE 1—*Continued.*

Hybrid Diffusion Model

$$C(t) = \frac{k_1}{V}\left\{\frac{1}{k_2} + \sum_{i=1}^{4}(\theta_i + \sqrt{k} + k_4/\theta_i)e^{\theta_i^2 t}\,\mathrm{erfc}(-\theta_i\sqrt{t})\Big/\prod_{\substack{j=1\\ j\neq i}}^{4}(\theta_i - \theta_j)\right\} - \frac{k_1}{V}\left\{\frac{1}{k_2} + \sum_{i=1}^{4}(\theta_i + \sqrt{k} + k_4/\theta_i)e^{\theta_i^2(t-t_o)}\,\mathrm{erfc}(-\theta_i\sqrt{t-t_o})\Big/\prod_{\substack{j=1\\ j\neq i}}^{4}(\theta_i - \theta_j)\right\} I_{(t_o,\infty)}(t)$$

$$+ C_0\sum_{i=1}^{4}\theta_i(k_4 + \sqrt{k}\,\theta_i + \theta_i^2)e^{\theta_i^2 t}\,\mathrm{erfc}(-\theta_i\sqrt{t})\Big/\prod_{\substack{j=1\\ j\neq i}}^{4}(\theta_i - \theta_j) + W_0\frac{k_4}{V}\sum_{i=1}^{4}\theta_i e^{\theta_i^2 t}\,\mathrm{erfc}(-\theta_i\sqrt{t})\Big/\prod_{\substack{j=1\\ j\neq i}}^{4}(\theta_i - \theta_j).$$

$$W(t) = k_1k_3\left\{\frac{1}{k_2k_4} + \sum_{i=1}^{4}e^{\theta_i^2 t}\,\mathrm{erfc}(-\theta_i\sqrt{t})/[\theta_i\prod_{\substack{j=1\\ j\neq i}}^{4}(\theta_i - \theta_j)]\right\} - k_1k_3\left\{\frac{1}{k_2k_4} + \sum_{i=1}^{4}e^{\theta_i^2(t-t_o)}\,\mathrm{erfc}(-\theta_i\sqrt{t-t_o})/[\theta_i\prod_{\substack{j=1\\ j\neq i}}^{4}(\theta_i - \theta_j)]\right\} I_{(t_o,\infty)}(t)$$

$$+ C_0k_3V\sum_{i=1}^{4}\theta_i e^{\theta_i^2 t}\,\mathrm{erfc}(-\theta_i\sqrt{t})\Big/\prod_{\substack{j=1\\ j\neq i}}^{4}(\theta_i - \theta_j) + W_0\sum_{i=1}^{4}\theta_i(k_2 + k_3 + \theta_i^2)e^{\theta_i^2 t}\,\mathrm{erfc}(-\theta_i\sqrt{t})\Big/\prod_{\substack{j=1\\ j\neq i}}^{4}(\theta_i - \theta_j).$$

$$Z(t) = k_1k_3\sqrt{k}\left\{\frac{2\sqrt{t/\pi}}{k_2k_4} - \frac{(k_2+k_3)\sqrt{k}}{k_2^2k_4^2} + \sum_{i=1}^{4}\frac{e^{\theta_i^2 t}\,\mathrm{erfc}(-\theta_i\sqrt{t})}{\theta_i^2\prod_{\substack{j=1\\ j\neq i}}^{4}(\theta_i - \theta_j)}\right\} - k_1k_3\sqrt{k}\left\{\frac{2\sqrt{(t-t_o)/\pi}}{k_2k_4} - \frac{(k_2+k_3)\sqrt{k}}{k_2^2k_4^2} + \sum_{i=1}^{4}\frac{e^{\theta_i^2(t-t_o)}\,\mathrm{erfc}(-\theta_i\sqrt{t-t_o})}{\theta_i^2\prod_{\substack{j=1\\ j\neq i}}^{4}(\theta_i - \theta_j)}\right\} I_{(t_o,\infty)}(t)$$

$$+ C_0k_3V\sqrt{k}\sum_{i=1}^{4}e^{\theta_i^2 t}\,\mathrm{erfc}(-\theta_i\sqrt{t})\Big/\prod_{\substack{j=1\\ j\neq i}}^{4}(\theta_i - \theta_j) + W_0\sqrt{k}\sum_{i=1}^{4}(k_2 + k_3 + \theta_i^2)e^{\theta_i^2 t}\,\mathrm{erfc}(-\theta_i\sqrt{t})\Big/\prod_{\substack{j=1\\ j\neq i}}^{4}(\theta_i - \theta_j) + Z_0.$$

$$U(x,t) = \frac{k_1k_3}{\lambda}\left\{\frac{\mathrm{erfc}[x/(2\sqrt{kt})]}{k_2k_4} + \sum_{i=1}^{4}\frac{e^{-x\theta_i/\sqrt{k}+\theta_i^2 t}\,\mathrm{erfc}[x/(2\sqrt{kt})-\theta_i\sqrt{t}]}{\theta_i\prod_{\substack{j=1\\ j\neq i}}^{4}(\theta_i - \theta_j)}\right\} - \frac{k_1k_3}{\lambda}\left\{\frac{\mathrm{erfc}[x/(2\sqrt{k(t-t_o)})]}{k_2k_4} + \sum_{i=1}^{4}\frac{e^{-x\theta_i/\sqrt{k}+\theta_i^2(t-t_o)}\,\mathrm{erfc}[x/(2\sqrt{k(t-t_o)})-\theta_i\sqrt{t-t_o}]}{\theta_i\prod_{\substack{j=1\\ j\neq i}}^{4}(\theta_i - \theta_j)}\right\} I_{(t_o,\infty)}(t)$$

$$+ C_0\frac{k_3V}{\lambda}\sum_{i=1}^{4}\theta_i e^{-x\theta_i/\sqrt{k}+\theta_i^2 t}\,\mathrm{erfc}[x/(2\sqrt{kt})-\theta_i\sqrt{t}]\Big/\prod_{\substack{j=1\\ j\neq i}}^{4}(\theta_i - \theta_j) + \frac{W_0}{\lambda}\sum_{i=1}^{4}(k_2 + k_3 + \theta_i^2)\theta_i e^{-x\theta_i/\sqrt{k}+\theta_i^2 t}\,\mathrm{erfc}[x/(2\sqrt{kt})-\theta_i\sqrt{t}]\Big/\prod_{\substack{j=1\\ j\neq i}}^{4}(\theta_i - \theta_j).$$

where $\theta_1,\ldots,\theta_4$ solve $\theta^4 + \sqrt{k}\,\theta^3 + (k_2+k_3+k_4)\,\theta^2 + (k_2 + k_3)\sqrt{k}\,\theta + k_2k_4 = 0$[c].

[a] Both real and negative.

[b] Both real and negative or complex conjugates.

[c] Real and negative or complex conjugates in pairs.

TABLE 2—*Summary of VOC sink data sets supplied by USEPA/AEERL.*

Data Set	VOC	A, m^2	V, m^3	k_1, μg/h	k_2, h^{-1}	n^a	Test Duration, h
Pillow-1	Ethylbenzene	0.266	0.0456	388.6	0.992	70	366.98
Pillow-2	Ethylbenzene	0.266	0.0456	330.6	0.955	70	366.97
Pillow-7	Perchloroethylene	0.266	0.0456	1196	0.923	115	167.75
Pillow-8	Perchloroethylene	0.266	0.0456	1208	0.925	105	165.75
Carpet-1	Ethylbenzene	0.14	0.053	432.6	0.949	80	408.08
Carpet-2	Ethylbenzene	0.14	0.0509	396.9	0.951	78	408.07

[a]Number of separate determinations in data set.

defines the mass in the interior of the sink at time t, and $U(x, t)$ is defined by the 1-dimensional diffusion (Eq 5). Equating Eq 15 to zero and solving for W defines the corresponding adsorption isotherm. From

$$\frac{dC}{dt} = \frac{1}{V}\frac{d(X - Y - W - Z)}{dt}$$

$$\frac{dC}{dt} = \frac{G(t)}{V} - (k_2 + k_3)C(t) - \frac{kA}{V}U_x(+0, t) + \frac{k_4}{V}W(t) - \frac{A}{V}\int_0^\infty U_t(x, t)dx \tag{17}$$

Initial condition #1 and boundary condition #2 were taken as in Eqs 9 and 10. With flux across the interface now proportional to the difference between inner and outer sink concentrations, boundary condition #3 became

$$kU_x(+0, t) = E[U(+0, t) - W/A] \tag{18}$$

so that $\lim_{E\to\infty} \frac{kU_x(+0, t)}{E} = 0$ suggested a second boundary condition, namely

$$\#3\ U(+0, t) = W/A \tag{19}$$

Table 1 gives solutions $C(t)$, $W(t)$, $Z(t)$, and $U(x, t)$ in terms of the complementary error function, usually with complex argument.

Methods of Model Validation

Six data sets, supplied by the Indoor Air Test Laboratory, Environmental Protection Agency/Air and Energy Engineering Research Laboratory (USEPA/AEERL) were used for model validation. Experimental details were described in Ref 5, and analyses based on the linear isotherm model were given there. The basic setup was 0.055 m^3 continuous flow test chambers with internal mixing fans. Critical details of individual tests are given in Table 2. The pillow material was described as "50% polyester-50% cotton fabric covering a polyester fiber fill," while the carpet material was described as "nylon fiber pile bound with styrenebutadiene latex to a jute backing." In all cases, input of VOC was terminated at t_0 = 48 h. Inspection of Table 2 will show that each successive pair of tests (Pillow-1 and Pillow-2, Pillow-7 and Pillow-8, Carpet-1 and Carpet-2) essentially were replications of each other.

All models were fitted to all data sets using least squares, as implemented by SAS procedure NLIN [*12*]. Necessarily, we were forced to write our own complex arithmetic routines in order to

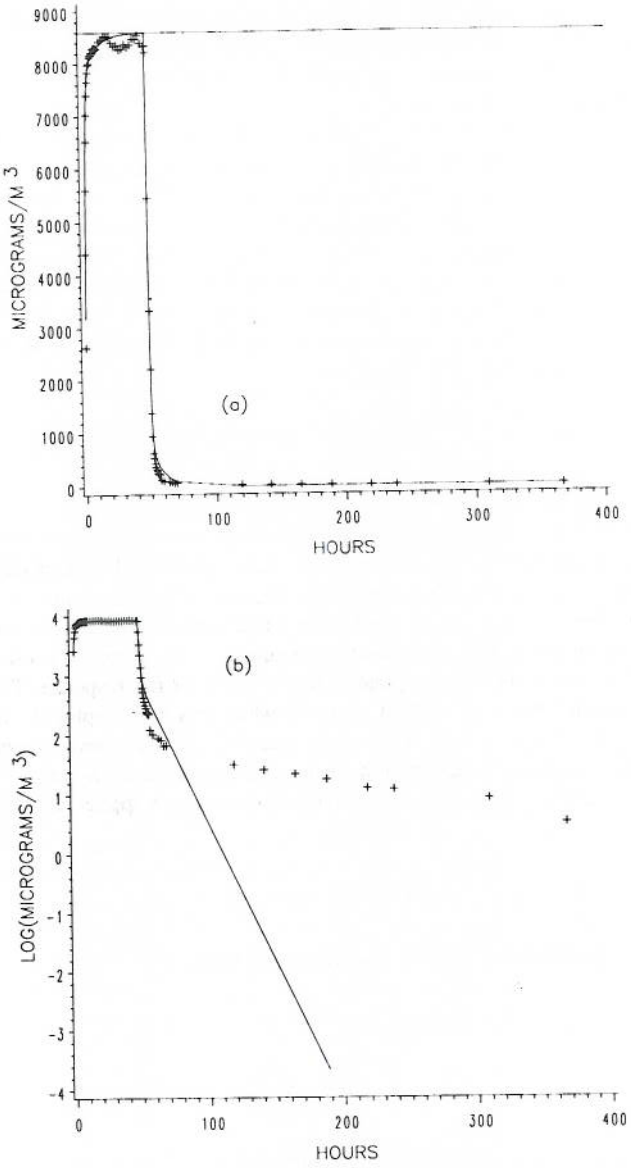

FIG. 2—*Fidelity of the Langmuir model to the Pillow-1 data. (a) Least squares fit of concentration in linear scale, and (b) least squares fit replotted in* $\log_{10}$ *scale of concentration.*

do so. The logical alternative, Fortran-based IMSL, was no more amenable in that the Fortran complementary error function does not accept a complex argument.

Figure 2(*a*) shows the fit of the linear isotherm model to the Pillow-1 data set. The solid curve represents the fitted model, while plus (+) represents an experimental determination. Concentration is expressed as $\mu g/m^3$. The horizontal line at 8591 $\mu g/m^3$ represents ultimate concentration given by $k_1/(k_2V)$, had the VOC source not been terminated. The fit looks quite good until replotted in Figure 1(*b*) in terms of log-concentration.

The problem is two-fold. First, Figure 2(*a*) represents a "point-weighted" (PW) fit in the sense that each data point has been given equal weight in determining the shape of the fitted curve. But since by choice, the technician sampled more frequently during the early stage of the experiment when chamber concentration was changing rapidly (consistent with good laboratory practice), this unequally weighted the influence of the passage of time on the fit. The solution, we felt, was to concentrate on the fact that each experiment produced one continuous response over time. That the technician took n determinations of chamber concentration at discrete times, $t_1, \ldots, t_n$, does not alter the conclusion. In order to compensate for the lack of continuous observation, we introduced an "interval weight" for each data point

$$w_i = (t_i - t_{i-1})/2 + (t_{i+1} - t_i)/2, \quad i = 1, \ldots, n-1$$

$$w_n = (t_n - t_{n-1})/2 \tag{20}$$

which reflects the amount of the experimental time axis represented by that data point, and performed all subsequent model fits using "interval-weighted" (IW) least squares.

The second problem stems from an increase in experimental error that is associated with increasing VOC concentration. This is evident in Figure 2(*a*), where more scatter of data appears about the trend line above 8000 $\mu g/m^3$ than at lower levels of the response. To compensate, we utilized the "transform both sides" (TBS) approach which has been explored extensively by Carroll and Ruppert [*13*]. Based on their method, let c_i and $C(t_i; \theta)$ represent, respectively, observed and theoretical VOC chamber concentrations at time t_i, and let $\lambda \geqq 0$ denote a parameter to be estimated in addition to (possibly vector-valued) θ. To do so, we applied IW least squares to the model

$$c_i^{\lambda} = C(t_i; \theta)^{\lambda} + e_i, \quad i = 1, \ldots n, \tag{21}$$

where e_i represents experimental error in the ith determination.

A practical implication of this model is that

$$\text{variance}[c_i] \propto C(t_i; \theta)^{2(1-\lambda)} \tag{22}$$

that is, the experimental error increases at a rate proportional to the $1 - \lambda$ power of the expected concentration. A value $\lambda = 0$ corresponds to a logarithmic transformation and implies a constant coefficient of variation.

Following Ref 13, we used IW least squares and TBS to fit all models in Table 1 to all data sets in Table 2 for equally spaced increments of λ over a range $0 \leqq \lambda \leqq 0.8$. By this approach, choice of λ reduced to maximizing the following, conditional log-likelihood function of λ, under the assumption that the experimental errors in Eq 21 are independent and normal with mean zero and variance σ^2

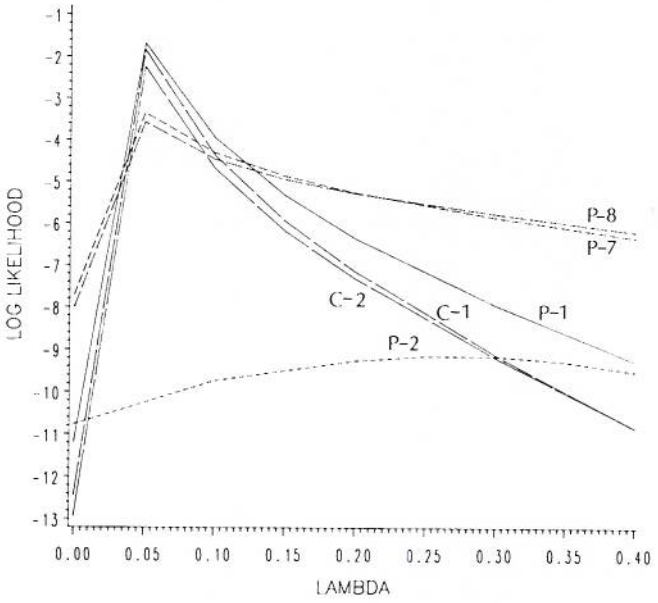

FIG. 3—*Log-likelihood plots to determine the optimal TBS power transformation when fitting the* K*-diffusion model to all data sets;* P = *pillow,* C = *carpet.*

$$L\{\lambda|\hat{\theta}\} = \sum_{i=1}^{n} w_i[(\lambda - 1)\ln(c_i) - 0.5\ \ln\{\mathrm{SSE}(\lambda)\}] \tag{23}$$

where $\mathrm{SSE}(\lambda) = \Sigma_{i=1}^{n}\, w_i[c_i^{\lambda} - C\{t_i;\ \hat{\theta}(\lambda)\}]^2$ and $\hat{\theta}(\lambda)$ denotes estimates of the model parameters conditional on λ. Figure 3 is representative of the results obtained. In this case, the *K*-diffusion model was fitted to each of the data sets in Table 2 using $\lambda = 0$, that is, TBS using a logarithmic transformation. Figure 3 shows a plot of $L\{\lambda|\hat{\theta}\ (\lambda = 0)\}$ for each of the six data sets. With the exception of the Pillow-2 data set (*P*-2), maximum *L* occurred in the region of $0 \leqq \lambda \leqq 0.05$. We considered this, and similar plots, which resulted by fitting the other models, to be sufficient evidence to base all comparisons of model validity in the following section on TBS using a logarithmic transformation ($\lambda = 0$). We did not feel justified in individual "tuning" of λ for each data set. If λ reflects the magnitude of experimental error, as suggested by Eq 22, then it should be relatively constant under conditions of constant test apparatus and quality of laboratory technique.

Results

Pillow Material Challenged with Ethylbenzene

Chamber conditions underlying the Pillow-1 and 2 data sets were the least well replicated, varying from 41 to 33% relative humidity, 22.7 to 23.1°C, and k_1 = 389 to 331 μg/h, respectively. Nevertheless, results presented in Table 3 were reproducible between replications for each of the models, with the exception of k in the hybrid model.

MSE is an estimator of σ^2 in the context of Eq 21, and is a measure of lack-of-fit. D.f. in Table 3 refers to the degrees of freedom associated with MSE. Based on this criterion, both the linear

TABLE 3—*Results Units:* $k = m^2/100\ h$, k_3 *and* $k_4 = (100\ h)^{-1}$.

Units: $k = m^2/100$ h, k_3 and $k_4 = (100\ h)^{-1}$.	
Pillow-1	Pillow-2
Linear Isotherm Model	
k_3 = 2.363, s.e. = 0.0859	2.408, s.e. = 0.0726
k_4 = 0.9284, s.e. = 0.0314	0.9084, s.e. = 0.0311
MSE = 9.23E-4 (68 d.f.)	6.45E-4 (65 d.f.)
K-diffusion Model	
k = 0.1930, s.e. = 0.0159	0.2114, s.e. = 0.0190
MSE = 1.99E-3 (69 d.f.)	2.16E-3 (66 d.f.)
Hybrid Diffusion Model	
k_3 = 3.442, s.e. = 0.213	3.811, s.e. = 0.196
k_4 = 1.748, s.e. = 0.277	1.990, s.e. = 0.352
k = 0.980, s.e. = 0.559	2.485, s.e. = 1.293
MSE = 7.41E-4 (67 d.f.)	3.09E-4 (64 d.f.)
Pillow-7	Pillow-8
Linear Isotherm Model	
k_3 = 3.596, s.e. = 0.141	4.155, s.e. = 0.203
k_4 = 2.180, s.e. = 0.0888	2.152, s.e. = 0.112
MSE = 3.13E-4 (103 d.f.)	4.87E-4 (103 d.f.)
K-diffusion Model	
k = 0.2190, s.e. = 0.00667	0.2989, s.e. = 0.0103
MSE = 1.04E-4 (104 d.f.)	1.24E-4 (104 d.f.)
Hybrid Diffusion Model	
k_3 = 15.17, s.e. = 4.25	59.17, s.e. = 22.2
k_4 = 45.36, s.e. = 19.7	304.0, s.e. = 161.7
k = 109.6, s.e. = 69.1	417.6, s.e. = 143.7
MSE = 4.35E-5 (101 d.f.)	1.24E-4 (102 d.f.)
Carpet-1	Carpet-2
Linear Isotherm Model	
k_3 = 3.331, s.e. = 0.289	3.770, s.e. = 0.942
k_4 = 1.405, s.e. = 0.0552	1.453, s.e. = 0.0547
MSE = 3.85E-3 (77 d.f.)	3.75E-3 (76 d.f.)
K-diffusion Model	
k = 0.6243, s.e. = 0.0647	0.6576, s.e. = 0.0782
MSE = 3.59E-3 (78 d.f.)	4.72E-3 (77 d.f.)
Hybrid Diffusion Model	
k_3 = 9.466, s.e. = 0.00054	13.09, s.e. = 0.311
k_4 = 4.831, s.e. = 0.152	5.766, s.e. = 0.0685
k = 0.3120, s.e. = 0.0385	0.3427, s.e. = 0.0326
MSE = 3.89E-4 (76 d.f.)	3.36E-4 (75 d.f.)

isotherm and the hybrid models gave superior fits compared to that of the *K*-diffusion model. Figures 4(*a*) to 4(*c*) demonstrate model adequacy in the logarithmic scale in which fitting occurred. Both linear isotherm and hybrid models cope very well with the sharp elbow that appeared late in the decay curve. By contrast, the *K*-diffusion model anticipated a longer period of VOC emissions and overestimated this part of the decay curve. Figures 4(*d*) to 4(*f*) show the same fitted models plotted in the original units of concentration. Clearly, fidelity to the decay phase on the part of both the linear isotherm and hybrid models left something to be desired during the accumulation phase. (Recall that both IW and fitting in the log scale tend to discount the early, large values.) Nevertheless, choice is between the linear isotherm and hybrid models. We prefer the former, since the large relative standard errors of k estimates for the hybrid model (57 and 52%, respectively) suggest that this may be a superficial parameter. Certainly, iterative convergence when fitting the hybrid model was slow to attain, and this often is indicative of an over-parameterized model.

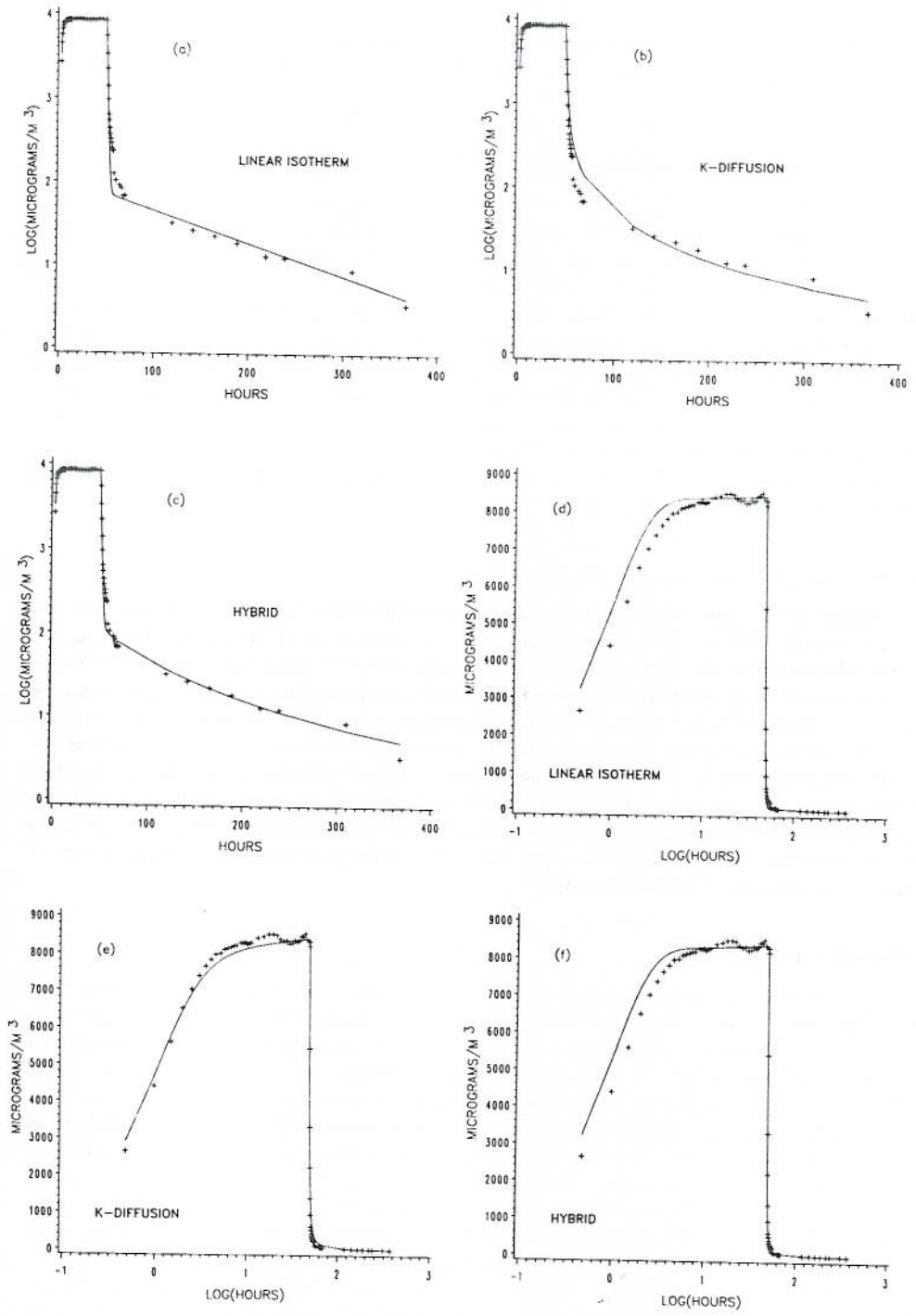

FIG. 4—*IW least squares model fits to pillow/ethylbenzene test chamber data (Pillow-1) in log_{10} scale of concentration, Figs. (a) through (c), and replotted in linear scale of concentration, Figs. (d) through (f).*

Therefore, we concluded that the sink effect of pillow material for ethylbenzene was dominated by thin-film, sorption phenomena, with insufficient evidence to identify a diffusion phenomenon as well.

Pillow Material Challenged with Perchloroethylene

Chamber conditions were well replicated in this case, being identically 45% relative humidity and 23.0°C, with k_1 = 1196 and 1208 μg/h, respectively. Figures 5(*a*) to 5(*f*) clearly demonstrate superior fits by the *K*-diffusion and hybrid models over that of the linear isotherm model. This is reinforced by a comparison of MSEs in Table 3. Here, the sharp elbow in the linear isotherm model decay curve works to its disadvantage. A choice of the *K*-diffusion model over the hybrid model is dictated by: (1) almost identical fits shown in the figures, (2) little reduction in MSE by adding sorption parameters, k_3 and k_4, in the presence of a diffusion term, (3) large relative standard errors for parameter estimates in the hybrid model, and (4) lack of reproducibility between replicates when fitting the hybrid model. Both (3) and (4) are indicative of an over-parameterized model. Since a sorption phenomenon seems to be ruled out by Fig. 5(*a*), we concluded that the sink effect of pillow material for perchloroethylene was dominated by a diffusion phenomenon with little evidence of a sorption/desorption effect.

Carpet Material Challenged with Ethylbenzene

Chamber conditions for the two replications were identically 43% relative humidity, 22.8 and 23.2°C, and k_1 = 433 and 397 μg/h, respectively. A comparison of Fig. 6(*c*) to Figs. 6(*a*) and 6(*b*) clearly demonstrates the superiority of the hybrid model over the linear isotherm and *K*-diffusion models during the decay phase. A comparison of MSEs in Table 3 also dictates a preference for the hybrid model. Relative standard errors of parameter estimates for the hybrid model were acceptably small, the estimates were reproducible between replicates, and iterative convergence was easily obtained for both data sets. In spite of poor fidelity to the data during the accumulation phase, as shown in Fig. 6(*f*), we concluded that the hybrid model had merit and that both diffusion and sorption/desorption phenomena were at play in the sink effect of carpet material in the presence of ethylbenzene. This is no surprise since the carpet material represents a complex mixture of natural and synthetic fibers and adhesive.

Discussion and Summary

The strongest case for the porous media, diffusion hypothesis was given by the excellent fit of the *K*-diffusion model to both pillow/perchloroethylene data sets. Even with only one adjustable parameter, *k*, the model fitted both the accumulation and decay phases very well even though data points during accumulation were heavily discounted by our fitting method. By contrast, the hybrid model fitted the decay phase of both carpet/ethylbenzene data sets very well, but its fidelity to the accumulation phase was less satisfactory. This places doubt on whether it truely is a unified model for this particular VOC/sink combination, since one would expect that a correct model fitted to one segment of the data should be able to predict any other segment of the data.

The apparent change in sink mechanism of pillow material that occurred when ethylbenzene was replaced by perchloroethylene is both interesting and puzzling. We believe the change over occurred, since it was reproducible, but its chemical basis escapes us.

Several worrisome details remain. The boundary condition of Eq 10 always has been suspect since it implies an infinitely deep sink. This is a standard heat equation assumption, but if it is to be replaced, with what? What does "depth" mean in terms of a pillow? Figure 7, based on parameters estimated from the excellent fit of the *K*-diffusion model to the Pillow-8 data set, is a

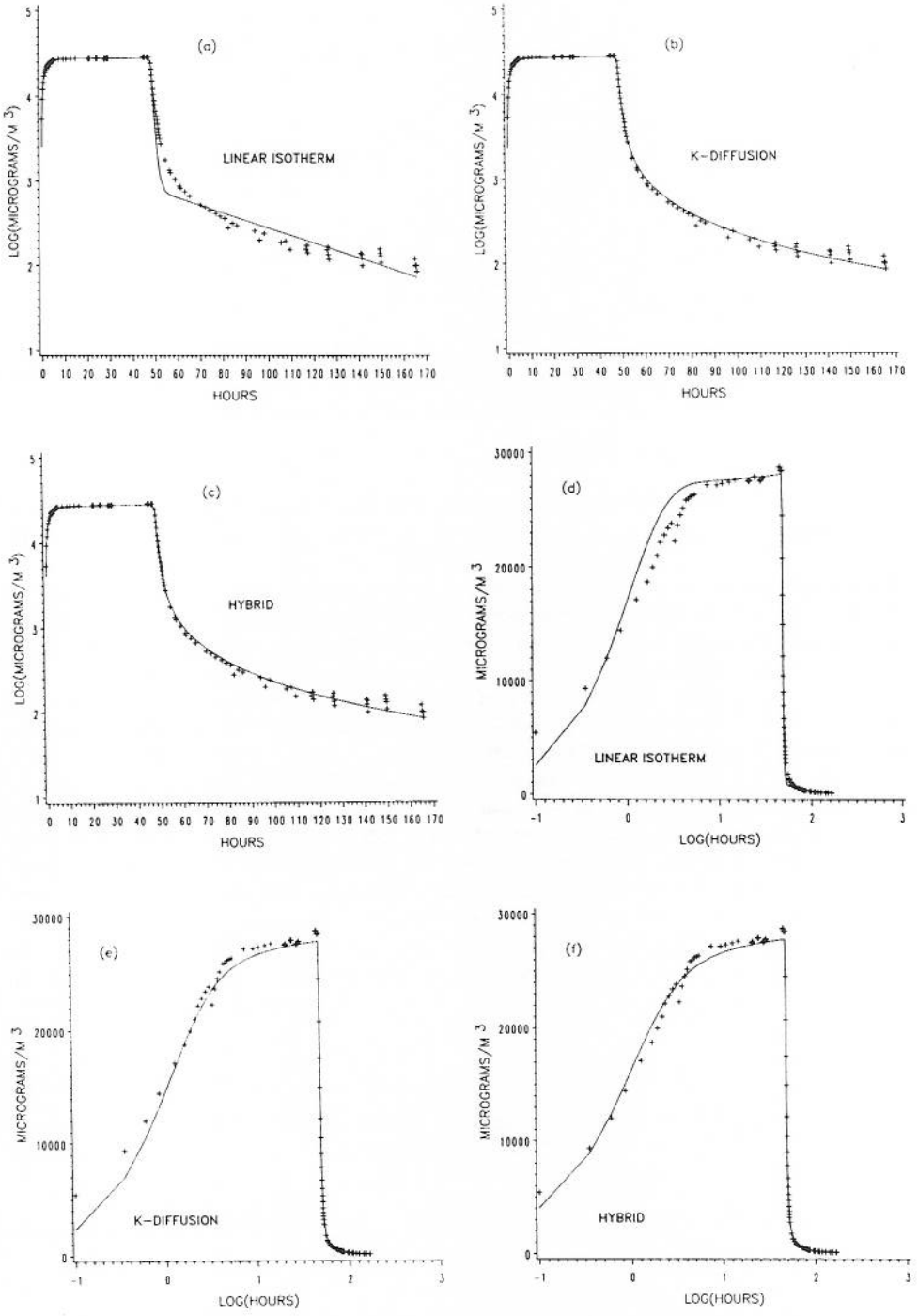

FIG. 5—*IW least squares model fits to pillow/perchloroethylene test chamber data (Pillow-8) in* $\log_{10}$ *scale of concentration, Figs. (a) through (c), and replotted in linear scale of concentration, Figs. (d) through (f).*

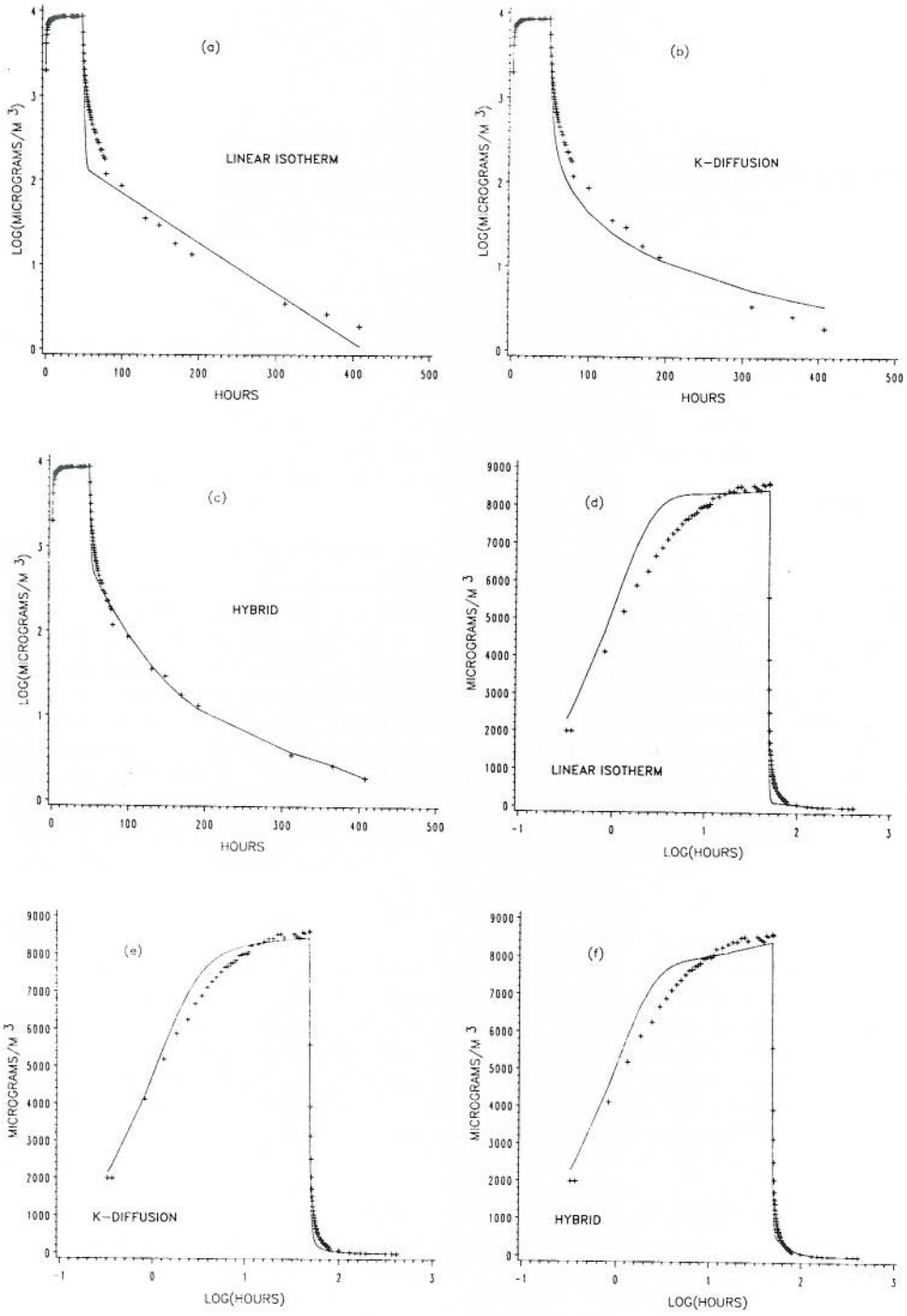

FIG. 6—*IW least squares model fits to carpet/ethylbenzene test chamber data (Carpet-1) in $\log_{10}$ scale of concentration, Figs. (a) through (c), and replotted in linear scale of concentration, Figs. (d) through (f).*

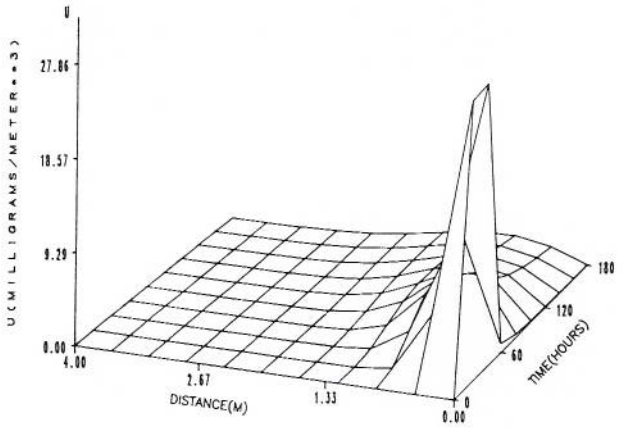

FIG. 7—*Estimated VOC concentration in the sink, based on the* K*-diffusion model fitted to the Pillow-8 data set.*

plot of VOC concentration as a function of distance of penetration into the sink and elapsed time. Can perchloroethylene molecules penetrate more than a meter into a pillow whose apparent thickness is only a few cm? This distance is suggestive of a diffusion pathway.

The diffusion-limited models presented here were developed because our interest was piqued by recalcitrant data sets resulting from pillow and carpet sorption studies and because of largely unsubstantiated speculation relating VOC emissions to porous diffusion. Because our confirmatory data was generated under dynamic test conditions, we largely focused on dynamic properties of the models. Steady-state properties, so familiar in adsorption science, were not useful in discriminating among the models. For example, $\lim_{t(<t_0)\to\infty} C(t) = k_1/(k_2 V)$ and $\lim_{t(>t_0)\to\infty} C(t) = 0$ for all three models characterized in Table 1. Admittedly, these models are not complete. So as to focus on dynamics, we defined models in terms of somewhat generic constants, then let data dictate the optimal choice of these constants, conditional on the dynamics of the model being correct. It is not implied that k_3, k_4, k, and E are global constants. They are assumed to be only locally constant within the course of an environmentally controlled experiment, and otherwise are dependent on temperature, chemical properties of the VOC, physical properties of the sink, and so forth. Clearly, the physical basis for these constants must be determined before the models have general application, say, in the building trades. Most recently, Guo and Tichenor [*11*] have illustrated an approach to VOC wet source modeling that combines both physical and chemical properties of the VOC with an experimental approach.

Acknowledgment

Research by the senior author was supported under the United States Environmental Protection Agency (US EPA) Cooperative Agreement CR–818520–01–0.

References

[*1*] Berglund, B., Johansson, I., and Lindvall, T., "Volatile Organic Compounds from Building Materials in a Simulated Chamber Study," *Environment International*, Vol. 15, 1989, pp. 383–388.

[*2*] Nielsen, P., "Potential Pollutants—Their Importance to the Sick Building Syndrome, and Their Release Mechanism," *Proceedings of Indoor Air '87*, Institute for Water, Soil, and Air Hygiene, Berlin, Vol. 2, 1987, pp. 598–602.

[3] Nielsen, P., "The Importance of Building Materials and Building Construction to the Sick Building Syndrome," *Proceedings of Healthy Buildings '88*, Swedish Council for Building Research, Stockholm, Vol. 3, 1988, pp. 391–399.

[4] Tichenor, B. A., Sparks, L. E., White, J., and Jackson, M., "Evaluating Sources of Indoor Air Pollution," Paper 88-110.2, presented at 81st Annual Meeting of the Air Pollution Control Association, Dallas.

[5] Tichenor, B. A., Guo, Z., Dunn, J. E., and Sparks, L. E., "The Interaction of Vapour Phase Organic Compounds with Indoor Sinks," *Indoor Air*, Vol. 1, 1991, pp. 23–35.

[6] Tichenor, B. A., "Indoor Air Sources: Using Small Environmental Test Chambers to Characterize Organic Emissions from Indoor Materials and Products," USEPA Report 600/8-89-074, U.S. Environmental Protection Agency, Washington, DC, 1989.

[7] DeBortoli, M. (co-coordinator), "Guideline for the Characterization of Volatile Organic Compounds Emitted from Indoor Materials and Products Using Small Test Chambers," Report 8, prepared by Working Group 8 of Community Cost Project 613, Commission of the European Communities.

[8] Dunn, J. E., "Models and Statistical Methods for Gaseous Emission Testing of Finite Sources in Well-mixed Chambers," *Atmospheric Environment*, Vol. 21, No. 2, 1987, pp. 425–430.

[9] Dunn, J. E. and Tichenor, B. A., "Compensating for Sink Effects in Emissions Test Chambers by Mathematical Modeling," *Atmospheric Environment*, Vol. 22, No. 5, 1988, pp. 885–894.

[10] Axley, J. W., "Adsorption Modeling for Building Contaminant Dispersal Analysis," *Indoor Air*, Vol. 2, 1991, pp. 147–171.

[11] Guo, Z. and Tichenor, B. A., "Fundamental Mass Transfer Models Applied to Evaluating the Emissions of Vapor-phase Organics from Interior Architectural Coatings," presented to the EPA/AWMA International Symposium on Measurement of Toxic and Related Air Pollutants, 3–8 May, Durham, NC, 1992.

[12] SAS Institute, Inc., *SAS User's Guide: Statistics*, Version 5, Cary, NC, 1985.

[13] Carroll, R. J. and Ruppert, D., "Power Transformations when Fitting Theoretical Models to Data," *Journal of the American Statistical Association*, Vol. 79, No. 386, 1984, pp. 321–328.